

Supporting Information

Zero-Field Slow Magnetic Relaxation of Zn₂Dy in a Family of Trinuclear Near Linear Zn₂Ln Complexes: Synthesis, Experimental and Theoretical Investigations

Naushad Ahmed,*^{a,b} and Kamal Uddin Ansari ^a

^a Dr. N. Ahmed and Dr. K. U. Ansari, Department of Chemistry, Indian Institute of Technology Bombay Powai, Mumbai-400076, Maharashtra, India. E-mail: naushad.chem@gmail.com (NA)

^b Current address: Department of Chemistry, Indian Institute of Technology Hyderabad, Kandi, Sangareddy, Telangana 502285, India.

Email. naushad.chem@gmail.com

Table S1. Crystallographic information table for the complexes **1_{-La}-6-Dy**

	1_{-La}	2_{-Ce}	3_{-Nd}	4_{-Sm}	5_{-Tb}	6_{-Dy}
Identification code	Zn ₂ Ce	Zn ₂ La	Zn ₂ Nd	Zn ₂ Sm	Zn ₂ Tb	Zn ₂ Dy
Empirical formula	C ₆₃ H ₆₃ CeN ₆ O ₂₁ Zn ₂	C ₆₃ H ₆₃ LaN ₆ O ₂₁ Zn ₂	C ₆₂ H ₅₉ N ₆ NdO ₂₀ Zn ₂	C ₆₂ H ₅₉ N ₆ O ₂₀ SmZn ₂	C ₆₂ H ₅₉ N ₆ O ₂₀ TbZn ₂	C ₆₂ H ₅₇ DyN ₆ O ₂₀ Zn ₂
Formula weight	1511.05	1509.84	1483.13	1489.24	1497.81	1499.37
Temperature/K	100.15	293(2)	150.00(10)	150.00(10)	273.15	150.00(10)
Crystal system	triclinic	triclinic	triclinic	triclinic	triclinic	mococlinic
Space group	P-1	P-1	P-1	P-1	P-1	C2/c
a/Å	12.693(3)	12.6542(8)	12.7538(3)	12.7211(10)	12.7840(16)	22.6246(16)
b/Å	13.251(3)	13.2334(8)	13.2632(3)	13.1975(11)	13.1615(17)	12.9505(6)
c/Å	21.930(6)	21.8815(9)	22.0875(3)	21.9778(12)	22.061(3)	24.2392(15)
$\alpha/^\circ$	86.0000(10)	85.739(4)	85.715(2)	85.982(6)	85.513(4)	90
$\beta/^\circ$	87.6080(10)	87.260(4)	87.298(2)	87.403(5)	87.341(4)	111.889(7)
$\gamma/^\circ$	61.616(6)	61.849(6)	61.566(3)	61.234(9)	61.328(4)	90
Volume/Å ³	3237.0(14)	3221.5(4)	3276.05(14)	3226.2(5)	3246.6(7)	6590.1(8)
Z	2	2	2	2	2	4
$\rho_{\text{calc}}/\text{g/cm}^3$	1.550	1.557	1.504	1.533	1.532	1.511
μ/mm^{-1}	1.507	1.470	1.583	1.713	1.887	1.920
F(000)	1538.0	1536.0	1506.0	1510.0	1516.0	3028.0
Crystal size/mm ³	0.14 × 0.12 × 0.1	0.12 × 0.09 × 0.08	0.032 × 0.025 × 0.021	0.021 × 0.015 × 0.01	0.25 × 0.034 × 0.021	0.025 × 0.023 × 0.021
Radiation	MoK α ($\lambda = 0.7107$)	MoK α ($\lambda = 0.71073$)	Mo K α ($\lambda = 0.71073$)	Mo K α ($\lambda = 0.71073$)	MoK α ($\lambda = 0.71073$)	Mo K α ($\lambda = 0.71073$)
2 θ range for data collection/ $^\circ$	6.138 to 53.998	4.124 to 52.744	3.498 to 50	3.526 to 49.998	3.884 to 49.998	3.696 to 49.996
Index ranges	-16 ≤ h ≤ 16, -16 ≤ k ≤ 16, -28 ≤ l ≤ 28	-15 ≤ h ≤ 15, -16 ≤ k ≤ 16, -27 ≤ l ≤ 27	-15 ≤ h ≤ 15, -15 ≤ k ≤ 15, -26 ≤ l ≤ 26	-15 ≤ h ≤ 15, -15 ≤ k ≤ 15, -26 ≤ l ≤ 26	-15 ≤ h ≤ 15, -15 ≤ k ≤ 15, -26 ≤ l ≤ 26	-26 ≤ h ≤ 26, -15 ≤ k ≤ 15, -28 ≤ l ≤ 27
Reflections collected	44546	42177	141581	141092	93955	56161
Independent reflections	14085 [R _{int} = 0.1054, R _{sigma} = 0.1159]	13160 [R _{int} = 0.0687, R _{sigma} = 0.0723]	11530 [R _{int} = 0.1016, R _{sigma} = 0.0472]	11347 [R _{int} = 0.1933, R _{sigma} = 0.0841]	11448 [R _{int} = 0.0583, R _{sigma} = 0.0333]	5801 [R _{int} = 0.0920, R _{sigma} = 0.0457]
Data/restraints/parameters	14085/18/857	13160/12/857	11530/6/836	11347/6/839	11448/148/861	5801/49/418
Goodness-of-fit on F ²	1.150	1.057	1.044	1.042	1.022	1.037
Final R indexes [I>=2σ (I)]	R ₁ = 0.0717, wR ₂ = 0.1303	R ₁ = 0.0509, wR ₂ = 0.1219	R ₁ = 0.0433, wR ₂ = 0.1015	R ₁ = 0.0527, wR ₂ = 0.1130	R ₁ = 0.0337, wR ₂ = 0.0751	R ₁ = 0.0499, wR ₂ = 0.1318
Final R indexes [all data]	R ₁ = 0.0861, wR ₂ = 0.1374	R ₁ = 0.0683, wR ₂ = 0.1359	R ₁ = 0.0622, wR ₂ = 0.1110	R ₁ = 0.0867, wR ₂ = 0.1277	R ₁ = 0.0463, wR ₂ = 0.0802	R ₁ = 0.0664, wR ₂ = 0.1443
Largest diff. peak/hole / e Å ⁻³	1.11/-1.03	0.62/-0.79	0.70/-0.78	0.65/-0.97	0.55/-0.58	1.05/-1.16

Table S2. Continuous Shape Measurement (CShM) analysis for Ln^{III} sites in **1_{-La}-6-Dy**

	1-La	2-Ce	3-Nd	4-Sm	5-Tb	6-Dy
DP-10	35.947	36.311	36.052	36.201	36.222	36.116
EPY-10	23.939	24.142	23.978	24.109	23.976	23.984
OBPY-10	11.684	15.093	14.971	14.867	14.767	14.905
PPR-10	11.684	11.686	11.947	12.006	12.183	12.299
PAPR-10	13.660	13.615	14.054	14.160	14.276	14.374
JBCCU-10	13.912	13.981	13.834	13.679	13.646	13.363
JBCSAPR-10	4.353	4.333	4.132	4.035	3.964	3.709
JMBIC-10	8.399	8.536	8.504	8.644	8.620	8.684
JATDI-10	16.755	16.966	16.920	17.079	17.309	17.283
JSPC-10	3.237	3.176	3.196	3.167	3.263	3.262
SDD-10	5.299	5.198	5.411	5.396	5.513	5.546
DP-10 D_{10h} Decagon, EPY-10 C_9 , Enneagonal pyramid, OBPY-10 D_{8h} Octagonal bipyramid PPR-10 D_{5h} Pentagonal prism, PAPR-10 D_{5d} Pentagonal antiprism, JBCCU-10 D_{4h} Bicapped cube J15 JBCSAPR-10 D_{4d} Bicapped square antiprism J17, JMBIC-10 C_{2v} Metabidiminished icosahedron J62 JATDI-10 C_{3v} Augmented tridiminished icosahedron J64, JSPC-10 C_{2v} Sphenocorona J87, SDD-10 D_2 Staggered Dodecahedron (2:6:2), TD-10 C_{2v} Tetradecahedron (2:6:2), HD-10 D_{4h} Hexadecahedron (2:6:2) or (1:4:4:1)						

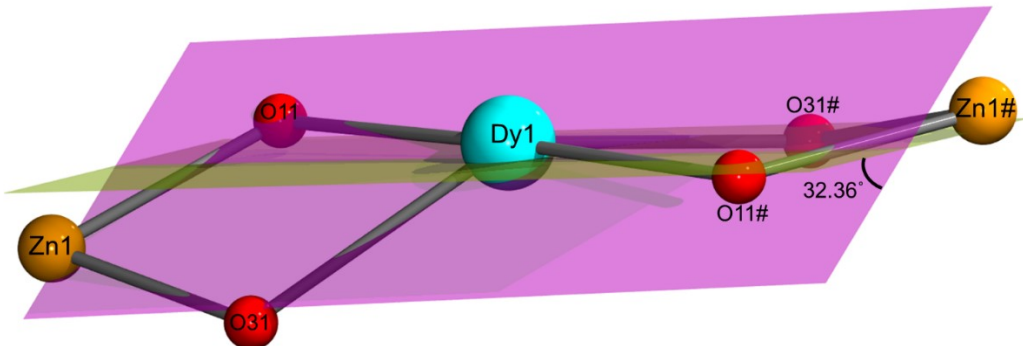


Figure S1. The twist between the two dihedral planes in **6-Dy**. The magenta and green planes consist of Zn1-O11-O31-Dy1 (plane 1) and Zn1#-O11#-O31#-Dy1 (plane 2) atoms respectively in **6-Dy**.

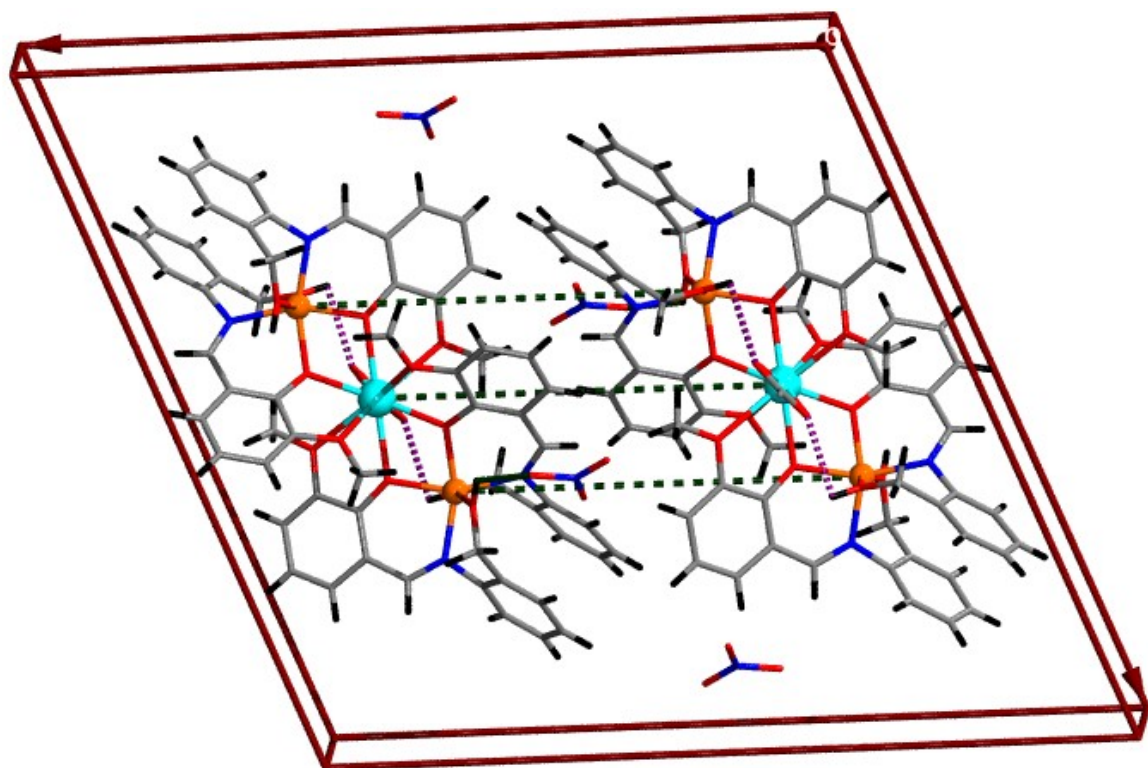


Figure S2. Packing structure of complex **6-Dy** projected along b-axis. Color code: Cyan = Dy^{3+} , orange = Zn^{2+} , red = O, blue= N, grey = C and black = H.

Table S3. Selected bond lengths and bond angle parameters for complexes **1_{-La}-6_{-Dy}**.

	1_{-La}	2_{-Ce}	3_{-Nd}	4_{-Sm}	5_{-Tb}	6_{-Dy}
Bond length (Å)						
Zn1-O11	2.042(4)	2.068(5)	2.095(3)	2.061(3)	2.049(2)	2.046(3)
Zn2-O51	2.002(4)	2.016(4)	2.044(2)	2.044(3)	2.018(3)	----
Zn1-O13	2.252(4)	2.262(4)	2.216(3)	2.331(3)	2.187(3)	2.340(4)
Zn2-O53	2.225(4)	2.227(4)	2.036(3)	2.280(3)	2.186(3)	-----
Zn1-O31	2.019(4)	2.040(4)	2.060(2)	2.016(3)	2.043(3)	2.030(3)
Zn2-O71	2.047(4)	2.075(4)	2.044(2)	2.027(3)	2.029(4)	----
Zn1-O33	2.283(4)	2.286(4)	2.328(3)	2.219(3)	2.229(3)	2.234(-3)
Zn2-O73	2.309(4)	2.227(4)	2.277(3)	2.271(3)	2.287(4)	-----
Zn1-N11	2.039(5)	2.045(5)	2.081(6)	2.036(4)	2.054(3)	2.039(4)
Zn2-N51	2.082(5)	2.045(5)	2.043(3)	2.044(3)	2.097(3)	----
Zn1-N31	2.071(5)	2.048(6)	2.036(3)	2.090(4)	2.084(3)	2.070(4)
Zn2-N71	2.025(5)	2.048(6)	2.072(3)	2.044(3)	2.046(3)	-----
Ln1-O11	2.562(4)	2.544(4)	2.653(3)	2.469(3)	2.054(3)	2.461(4)
Ln1-O12	2.687(4)	2.694(5)	2.596(3)	2.634(3)	2.590(3)	2.625(3)
Ln1-O31	2.428(4)	2.412(4)	2.492(2)	2.363(3)	2.695(3)	2.311(3)
Ln1-O32	2.710(4)	2.708(4)	2.642(2)	2.631(3)	2.439(2)	2.599(3)
Ln1-O51	2.431(4)	2.416(4)	2.518(2)	2.495(3)	2.717(3)	
Ln1-O52	2.689(4)	2.676(4)	2.660(2)	2.643(3)	2.443(2)	
Ln1-O71	2.523(4)	2.512(4)	2.386(2)	2.644(3)	2.679(3)	
Ln1-O72	2.663(4)	2.677(4)	2.674(2)	2.357(3)	2.552(3)	
Ln1-O92	2.556(4)	2.566(5)	2.518(3)	2.488(3)	2.572(3)	2.435(3)
Ln1-O93	2.579(4)	2.459(4)	2.521(3)	2.493(3)	2.585(3)	
Bond angle (°)						
Zn1-O11-Ln1	105.55(11)	105.77(11)	105.51(19)	106.67(18)	106.91(9)	106.24(9)
Zn2-O51-Ln1	112.030(9)	112.02(9)	111.61(10)	112.30(12)	112.27(9)	-----
Zn1-O31-Ln1	111.290(9)	112.59(12)	112.47(10)	112.29(19)	110.92(9)	112.52(10)
Zn2-O71-Ln1	106.97(13)	106.87(13)	106.15(10)	106.23(19)	106.56(9)	----
Dihedral angle(°)						
O31-Zn1-O11-Ln1	14.47(10)	14.20(10)	15.040(2)	13.96(20)	14.01(9)	14.85(16)
O71-Zn2-O51-Ln1	14.01(12)	14.09(12)	14.130(2)	13.82(20)	13.70(9)	-----
The twist angle between the two dihedral planes mentioned above (°)						
	30.51(11)	30.50(10)	31.493(2)	31.164(4)	29.57(6)	32.36(13)
Intramolecular interatomic distance (Å)						
Zn1-Ln1	3.679	3.689	3.66(1))	3.66(10)	3.699(4)	3.613(12)
Zn2-Ln1	3.684	3.693	3.65(1)	3.682(10)	3.771(4)	-----
Zn1-Zn2	7.339	7.539	7.29(2)	7.348(20)	7.388(8)	7.203(23)

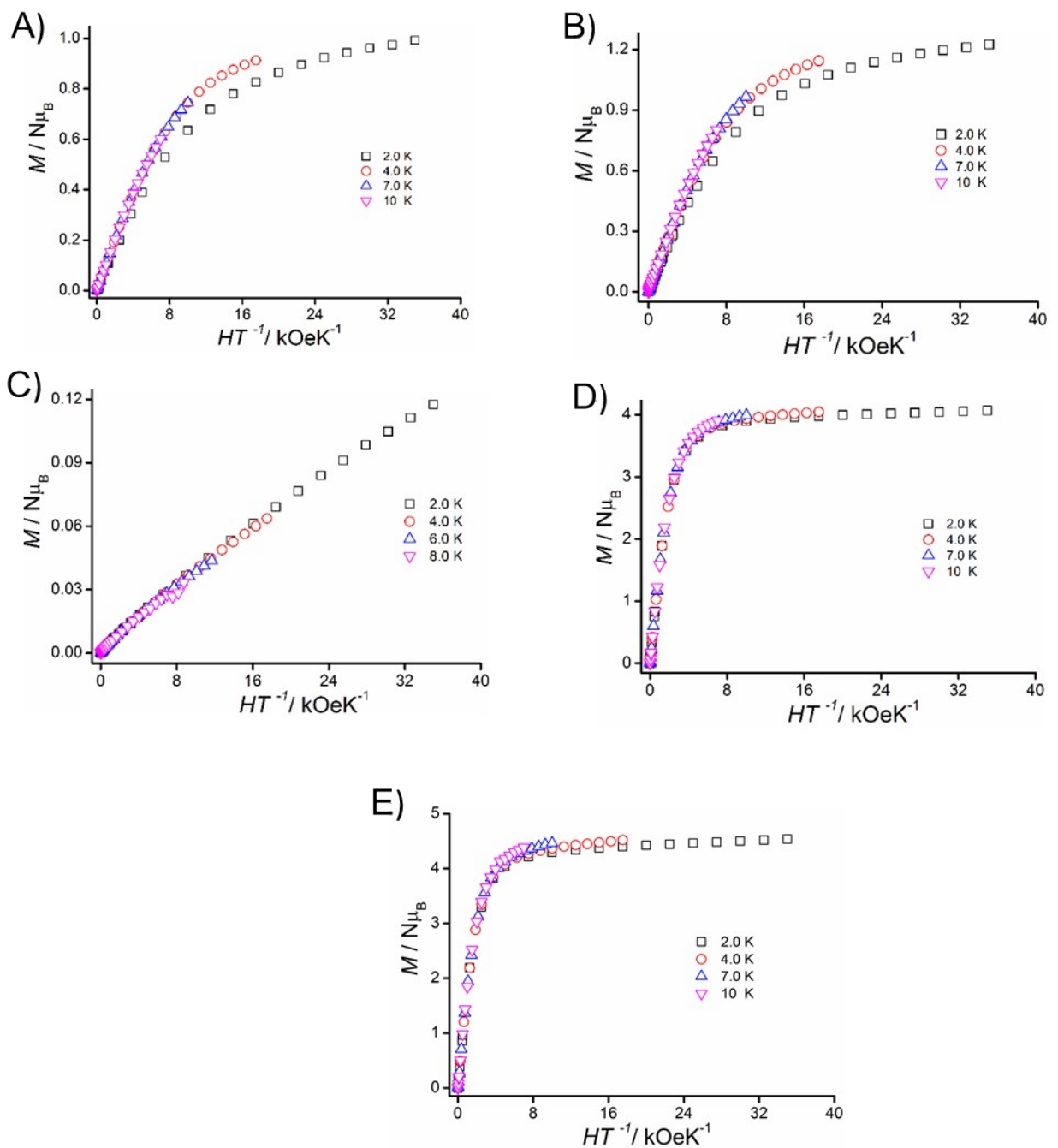


Figure S3. Reduced magnetization curves A-E for complexes **2-Ce-6-Dy** respectively.

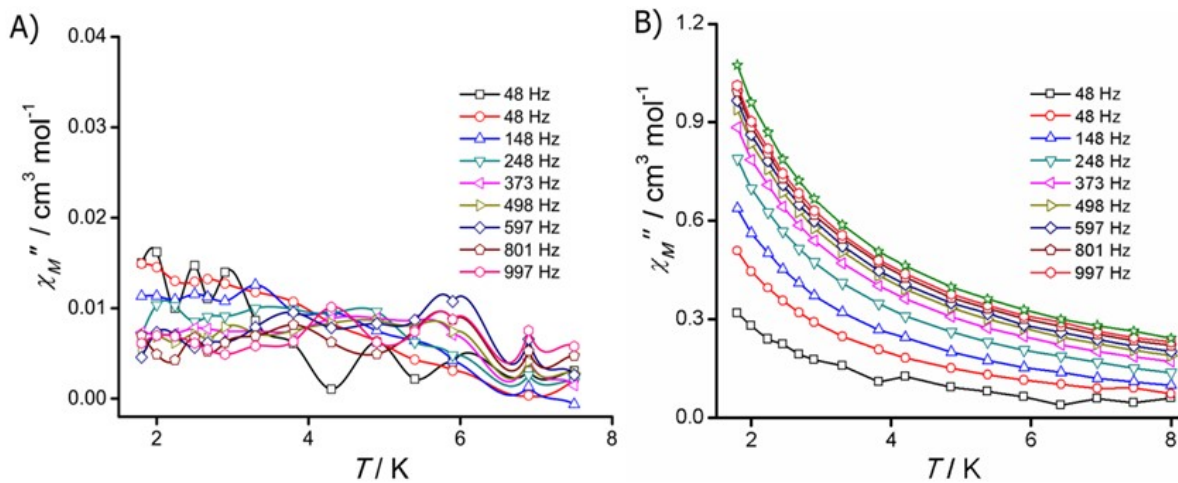


Figure S4. Alternating current out of phase magnetic susceptibility measurement performed at zero dc bias magnetic field and 3.5 Oe oscillating ac field for complexes **2-Ce** (A) and **5-Tb** (B) respectively.

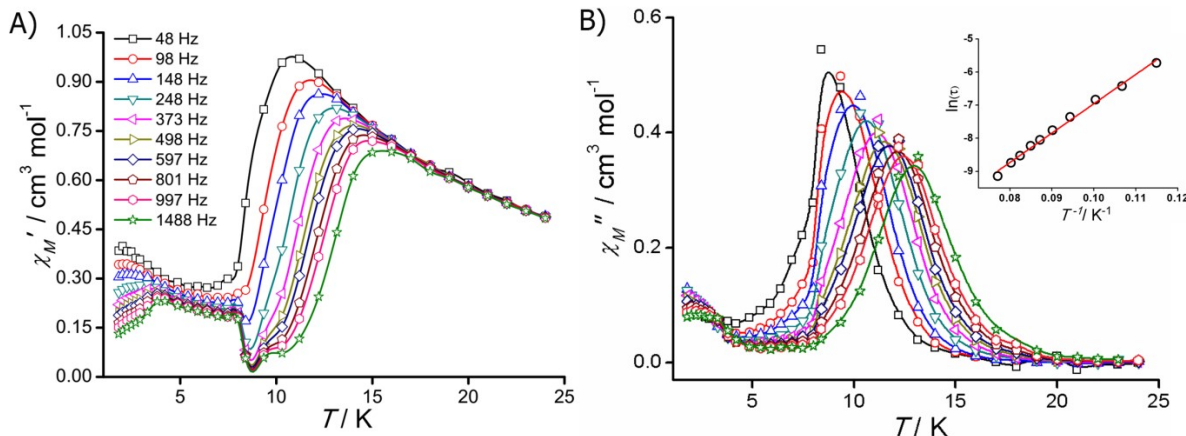


Figure S5. Alternating current magnetic susceptibility measurement at 2 kOe dc field and 3.5 Oe oscillating field for **6-Dy**. The frequency dependent in-phase and out-of-phase signals (A-B) respectively. Inset in panel B shows the Arrhenius fit to extract the energy barrier.

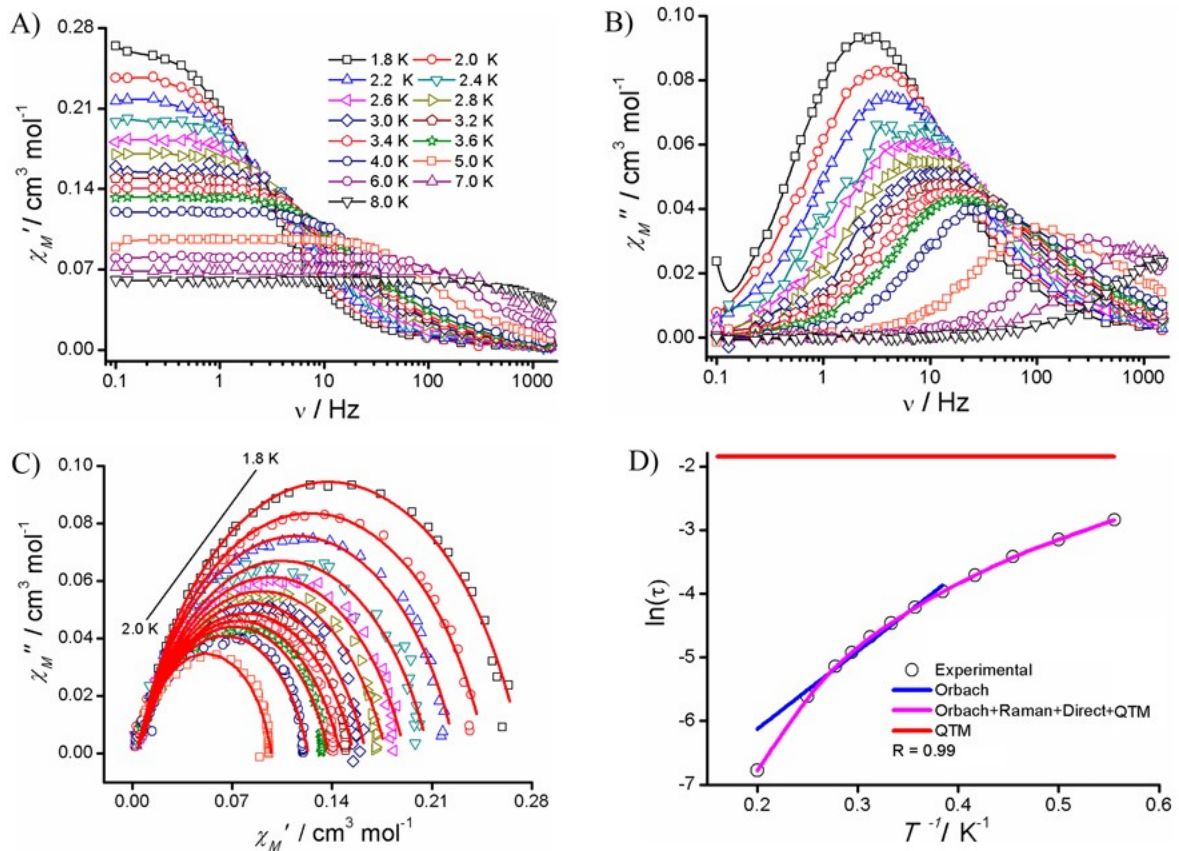


Figure S6. Alternating current magnetic susceptibility measurement at 2.0 kOe dc field and 3.5 Oe oscillating field for complex **2_{Ce}**. The frequency dependent in-phase and out-of-phase signals (A and B), Cole-Cole plot (C) and Arrhenius plot constructed from τ value obtained from Cole-Cole fit (D). Solid lines represent the fit with parameter describe in the text.

Table S4. Reported Zn₂Dy single-molecule magnets. If field applied it is given in the parenthesis.

S. No	Complex	U_{eff} (cm ⁻¹)(Oe)	τ_o (s)	References
1	[Dy(ZnL) ₂ (CH ₃ COO)Cl ₂]·CH ₂ Cl ₂ ^a	13.2(700)	9.1×10^{-6}	1
2	[(LZn(H ₂ O)) ₂ Dy(H ₂ O)][CF ₃ SO ₃] ^b	68.5	2.4×10^{-7}	2
		91.8	1.8×10^{-8}	
3	[(LZnBr) ₂ Dy(H ₂ O)][ClO ₄] ^b	104.8	9.2×10^{-8}	2
		153.3	9.8×10^{-9}	
4	[(LZnCl) ₂ Dy(H ₂ O)][ClO ₄]·1.25MeOH ^b	104.3	9.9×10^{-9}	2
		144.6	1.5×10^{-8}	
5	[Zn ₂ (L ₁) ₂ DyCl ₃].2H ₂ O ^c	307.1	7.4×10^{-11}	3
		343.6 (1000)	1.3×10^{-11}	
6	[Zn ₂ (L ₁) ₂ Dy(MeOH)Br ₃].3H ₂ O ^c	166.4	2.5×10^{-8}	3
7	[Zn ₂ (L ₁) ₂ Dy(H ₂ O)Br ₂].[ZnBr ₄] _{0.5} ^c	86.4	8.5×10^{-7}	3
8	[Zn ₂ (L ₂) ₂ DyCl ₃].2H ₂ O ^c	284.3	3.5×10^{-10}	3
9	[DyZn ₂ (Hhms) ₂ (C ₆ H ₅ COO) ₄] ^d ·C ₆ H ₅ COO ^e	8.7 (500)	1.01×10^{-6}	4
10	[Zn ₂ Dy(L ₁) ₂ (OAc) ₄](NO ₃) _{0.93} B _{0.08} ^f	25 (3000)	5.28×10^{-8}	5
11	[Zn ₂ Dy(L ₁) ₂ (OAc) ₄]ClO ₄ ^f	12.09 (1000)	5.8×10^{-9}	5
12	[Zn ₂ Dy(L ₁) ₂ (OAc) ₄]Cl ^f	14.08 (1000)	3.0×10^{-8}	5
13	[Zn ₂ Dy(L ₁) ₂ (OAc) ₄]PF ₆ ^f	55.5 (1000)	1.0×10^{-10}	5
14	[Zn ₂ Ln(HL) ₄ (NO ₃)].(NO ₃) ₂	30.37	2.42×10^{-6}	This Work

^aH₂L=N,N'- bis(3-ethoxysalicylidene)phenylene-1,2-diamine, ^bL= N,N'-2,2 dimethylpropylenedi(3-methoxysalicylideneiminato, ^cH₂L₂=N,N'-bis(3 methoxysalicylidene)-1,2-dia- minocyclohexane, ^dH₃L=6,6'-(((2-(5-bromo-2-hydroxy-3 methoxyphenyl)imidazolidine-1,3-diyl)bis(ethane-2,1 diyl))bis(azanylylidene))bis(methanylylidene))bis(4-bromo-2-methoxyphenol), ^eH₂hms(2 hydroxy-3-methoxybenzylidene)-semicarbazide, ^fL₁= 2-methoxy-6-((2 methoxyphenyl)imino)methyl)phenol.

Computational Details

The *ab initio* calculations were performed on the X-ray structures of the complexes **2-Ce-6-Dy** using MOLCAS 8.0 code. We have computed single-ion property of the lanthanide paramagnetic centre. In the complete active space self-consistent field (CASSCF) method we have considered the 1, 3, 5, 8 and 9 active electron(s) of Ce³⁺ (CAS(1,7)), Nd³⁺(CAS(3,7)), Sm³⁺(CAS(5,7)), Tb³⁺(CAS(8,7)) and Dy³⁺(CAS(9,7)) ion respectively spanning in seven *f*-orbitals orbitlas. Under the configuration integration method we have computed spin-free energy of the 7 doublets (for Ce³⁺), 112 doublets and 35 quartets (for Nd³⁺), 224 quartets and 21 sextets (for Sm³⁺ and Dy³⁺) and 140 quintets and 7 heptets (for Tb³⁺) excited states respectively in complexes **2-Ce-6-Dy**. The computed spin-free states were mixed in the spin-orbit restricted active space state interaction (SO-RASSI) step to obtain spin-orbit states. Due to the hardware limitation we have mixed only limited number of excited roots (128 quartets + 21 sextets) and (108 quartets + 21 sextets) for Sm³⁺ and Dy³⁺ respectively in the case of complexes **4-Sm** and **6-Dy**. Finally SINGLE_ANISO module used to compute the g-tensors, dc magnetic property and *ab initio* energy barrier for magnetic relaxation.

Table S5. Basis set used for elements for ab initio calculations using MOLCAS 8.0 program.

Element	Basis set
C	ANO-RCC...3s2p.
H	ANO-RCC...2s.
N , O	ANO-RCC...3s2p1d.
Zn	ANO-RCC...5s4p2d.
Ln	ANO-RCC...8s7p5d3f2g1h.

Table S6. The CASSCF computed energy (cm^{-1}) of the spin-free states for complex **2-Ce - 4-Sm**. The red values represent the 7 doublets (for Ce), 35 quartets (for Nd) and 21 sextets (for Sm) respectively. The grey values represent 112 doublets (for Nd) and 224 quartets (for Sm) respectively.

2-Ce	3-Nd				4-Sm					
0.000	0.000	19291.140	35539.442	87403.419	0.000	23171.638	28332.184	40883.343	69038.107	95261.460
46.366	21.444	19318.329	35675.163	87539.457	28.249	23194.691	28337.061	40922.107	69045.545	95316.848
214.810	66.975	19337.316	35677.562	87866.289	203.781	23199.034	28342.807	40945.422	69046.060	95463.275
304.021	69.164	19406.789	35806.318		250.160	23204.476	28355.142	40977.206	69096.372	95482.303
484.100	240.944	19418.158	35817.639		318.263	23225.052	28357.557	40992.959	69101.64	95490.975
625.810	254.662	19517.408	35952.583		587.425	23263.797	29870.959	51084.646	69153.752	
1446.672	401.788	19522.269	35992.396		601.763	23265.723	29886.497	51089.218	69164.361	
	450.466	21456.936	36080.823		651.858	23272.502	29922.673	51141.855	69216.408	
	615.002	21456.975	36145.493		691.977	23300.300	29934.444	51145.89	69218.606	
	672.194	21582.118	36215.369		824.355	23322.726	29992.256	51151.936	69233.025	
	726.733	21582.795	36241.655		827.686	23339.416	31093.801	51205.662	69288.612	
	895.595	21688.910	36270.379		7005.014	23421.236	31125.173	51327.628	69306.331	
	956.784	21690.786	39586.109		7013.050	23835.565	31129.121	51396.802	70268.345	
	14403.111	21831.121	39590.237		7112.689	23887.802	31204.641	51415.181	70499.299	
	14734.413	21834.094	39803.163		7165.037	23942.378	31205.201	51458.536	70527.105	
	14766.227	21959.135	39859.411		7196.146	24011.402	31340.838	51462.538	70639.890	
	14809.129	21980.401	39882.011		7198.853	24030.939	31342.316	51498.0774	70706.402	
	14811.149	22041.502	39888.904		7374.727	24094.249	31375.361	51527.379	70867.823	
	14878.721	22074.285	39965.400		31320.037	24098.702	31381.678	51550.639	70883.579	
	15003.502	22121.090	39992.668		31538.943	24162.167	31392.172	51579.215	76405.016	
	15019.872	22141.401	40031.896		32012.204	24163.039	31407.932	51611.727	76432.741	
	22662.634	22160.392	40075.615		22421.437	26745.507	33884.037	51619.933	76768.034	
	22695.971	26263.962	40094.173		22447.856	26774.732	34018.983	51638.116	76854.080	
	22972.657	26311.591	40667.635		22496.000	26834.642	34036.770	51815.420	76977.846	
	23029.741	26343.783	40737.947		22517.491	26838.707	34072.501	51816.864	78890.152	
	23054.219	26422.171	40941.329		22556.917	26864.840	34080.213	55519.211	78890.983	
	23120.301	26736.644	41036.575		22584.460	26885.164	34167.038	55519.362	78998.330	
	23207.083	26742.416	41201.458		22585.368	26908.541	34214.301	55586.616	79000.402	
	23272.981	26756.927	47996.109		22606.020	26920.954	34337.851	55586.676	79296.085	
	23370.334	26763.855	48057.898		22616.720	26946.108	34379.973	55759.635	79297.636	
	37099.275	34530.060	48095.550		22644.310	27005.564	34488.557	55760.764	79365.0704	
	37108.247	34530.471	48115.378		22659.428	27015.221	34528.403	55863.770	79372.288	
	37460.867	34733.382	48243.969		22669.497	27048.222	34585.656	55864.430	79414.504	
	37695.516	34735.071	48265.552		22677.449	27073.401	39132.907	55907.36	79444.059	
	37827.824	34823.796	48275.402		22687.172	27233.093	39170.606	55909.713	79469.805	
	14651.753	34842.313	60736.554		22728.064	27234.450	39261.474	55930.012	79610.031	
	14661.263	34884.762	60737.579		22739.981	28193.402	39343.779	55960.819	79623.654	
	14675.204	34944.081	60906.553		22791.015	28203.162	39428.200	55980.014	88449.103	
	14676.532	34954.178	60923.630		22811.658	28206.369	39499.757	56075.580	88467.559	
	14686.250	35033.504	61066.477		22900.464	28214.978	39918.091	56081.073	88638.576	
	14694.196	35044.819	61106.060		22934.262	28225.074	40548.181	60092.489	88703.137	
	14710.902	35056.498	61143.289		22939.024	28267.986	40548.963	60549.970	89002.779	
	14728.613	35075.813	61273.048		22966.484	28268.688	40777.571	60781.694	89009.982	
	14733.075	35216.958	61343.121		22970.911	28274.822	40782.231	65197.910	89097.043	
	14788.259	35224.252	86573.023		23004.627	28284.219	40800.368	65422.266	94957.645	
	14794.040	35425.474	86589.332		23128.001	28312.326	40802.699	65543.165	94964.192	
	19204.996	35426.842	87043.157		23151.941	28314.544	40820.710	65984.012	95210.475	
	19219.485	35539.053	87229.184		23155.093	28331.420	40839.421	66019.617	95230.049	

Table S7. The CASSCF computed energy (cm^{-1}) of the spin-free states for complexes **5-Tb** and **6-Dy**. The red values represent the 7 septets (for Tb) and 21 sextets (for Dy) and respectively. The grey values represent 140 quintets (for Tb) and 224 quartets respectively.

5-Tb				6-Dy				
0.000	270630.634	285579.395	324813.489	0.000	25658.897	31495.171	45654.433	77965.362
48.328	274206.933	285775.043	325768.964	3.630	25668.016	31496.828	45655.238	77971.553
271.843	274299.415	287543.910	325881.208	142.390	25676.457	31520.508	45867.109	77988.829
411.483	274479.028	287620.772		190.297	25688.302	31520.568	45867.166	77995.566
486.583	274605.801	288330.431		202.369	25716.352	33248.833	57779.330	78000.698
542.511	274654.876	290182.548		216.530	25756.141	33304.572	57796.134	78021.264
1010.497	274669.450	290230.850		421.906	25763.995	33311.185	57818.072	78024.903
261267.409	274684.937	290282.483		506.875	25777.133	33342.434	57829.818	78093.657
261282.620	274738.431	290386.989		543.108	25782.752	33378.466	57892.100	78094.077
261308.936	274810.412	290588.406		698.673	25955.655	34724.483	57904.244	78119.045
261421.096	274834.536	290650.569		704.465	25955.663	34732.733	57915.068	78120.484
261470.546	274924.917	290774.031		7616.940	26471.073	34757.201	57961.417	79425.596
264300.599	274982.185	291000.793		7753.389	26474.010	34760.167	57963.479	79433.173
264334.371	275047.014	291050.321		7773.030	26612.553	34773.565	58076.444	79544.187
264348.086	275073.189	291234.706		7805.886	26628.962	34796.172	58083.663	79597.969
264437.847	275112.345	291286.278		7840.754	26648.716	34881.561	58201.281	79770.090
264495.617	275181.674	300420.273		7909.582	26658.163	34891.351	58211.731	79786.722
264519.885	275220.860	306151.911		7917.740	26747.536	34952.777	58272.167	79908.965
264552.971	275350.406	306212.275		34734.280	26785.125	34958.611	58287.937	86171.052
264642.417	275405.151	306299.040		35251.745	26792.647	34964.897	58292.381	86278.693
264703.351	275412.639	306348.425		35413.120	29795.873	37860.334	58307.400	86377.915
264734.703	279233.968	306359.679		24987.800	29796.060	37974.464	58336.405	86733.878
264844.219	279235.624	306385.528		24989.421	29883.717	38053.716	58388.930	86742.015
264919.034	279570.142	306461.670		25011.461	29913.378	38066.903	58424.330	89079.801
264972.789	279621.169	306606.103		25011.863	29938.117	38077.241	62819.352	89099.276
265027.425	279662.672	306627.796		25114.309	29939.010	38129.647	62821.528	89181.371
265051.535	279681.726	306684.672		25121.452	29979.895	38167.830	62866.091	89204.200
265125.070	279782.149	306721.596		25156.234	30000.550	38204.058	62878.717	89220.652
265140.028	279881.351	306889.188		25160.676	30009.700	38362.398	62889.272	89259.986
265702.503	279907.375	306918.109		25194.131	30024.702	38365.522	62922.730	89268.823
265789.769	279985.522	308222.617		25201.200	30046.766	38406.942	62926.894	89380.467
266004.328	280051.115	308443.731		25252.766	30067.188	38415.652	62996.232	
266031.297	280080.494	308483.416		25258.569	30087.679	43665.886	62996.997	
266148.313	280104.559	308961.862		25272.876	30125.904	43897.790	63092.748	
266212.228	280193.059	308994.330		25295.723	30133.895	43929.375	63093.670	
266281.497	280228.534	309014.213		25385.280	31375.099	44030.038	63243.087	
266321.454	283450.523	309062.062		25390.552	31375.742	44072.802	63243.228	
266522.090	283491.672	321993.386		25426.541	31407.827	44143.519	63291.294	
269839.440	283556.504	322360.307		25454.899	31407.853	44170.638	63291.412	
269884.566	283644.063	322669.792		25482.274	31414.517	45417.906	68011.154	
270039.214	283713.206	322808.456		25487.415	31416.090	45421.853	68140.652	
270121.745	283851.802	322892.729		25492.497	31435.481	45475.652	68615.474	
270226.219	283911.402	323097.551		25499.524	31437.296	45485.343	73752.173	
270260.362	284005.377	323136.880		25536.273	31449.292	45525.134	73754.815	
270470.389	284019.460	324209.614		25536.297	31449.358	45540.706	74160.686	
270493.561	285042.371	324316.973		25555.864	31462.904	45551.941	74282.685	
270523.597	285120.981	324555.748		25565.425	31468.184	45586.789	74343.207	
270573.178	285457.510	324654.772		25573.292	31480.255	45588.312	77855.474	

Table S8. The CASSCF+SO-RASSI computed energy (cm^{-1}) of the low lying spin-orbit states for complexes **2-Ce** - **6-Dy**.

2-Ce	3-Nd	4-Sm	5-Tb	6-Dy
0.000	0.000	0.000	0.000	0.000
0.000	0.000	0.000	0.002	0.000
363.848	31.601	170.662	176.983	136.044
363.848	31.601	170.662	177.018	136.044
583.385	148.954	417.211	331.466	167.033
583.385	148.954	417.211	334.729	167.033
	403.028		407.565	227.976
	403.028		426.637	227.976
	428.000		450.353	343.738
	428.000		468.715	343.738
			488.660	439.811
			624.680	439.811
			628.180	512.536
				512.536
				580.605
				580.605

Table S9. SINGLE_ANISO computed wave function decomposition analysis for Ln(III) in complex **2-Ce** - **6-Dy**. The major dominating values are kept in bold.

$\pm m_J$	<i>wave function decomposition analysis</i>
2-Ce	
KD1	97.7% $ \pm 5/2\rangle$ + 1.2% $ \pm 1/2\rangle$ + 0.039% $ \pm 3/2\rangle$
KD2	44.1% $ \pm 3/2\rangle$ + 12.37% $ \pm 1/2\rangle$ + 0.5% $ \pm 5/2\rangle$
KD3	58.7% $ \pm 1/2\rangle$ + 26.4% $ \pm 3/2\rangle$ + 0.75% $ \pm 5/2\rangle$
3-Nd	
KD1	47.9% $ \pm 7/2\rangle$ + 24.3% $ \pm 9/2\rangle$ + 22.2% $ \pm 5/2\rangle$ + 3.3% $ \pm 1/2\rangle$
KD2	46.9% $ \pm 9/2\rangle$ + 25.3% $ \pm 5/2\rangle$ + 15.3% $ \pm 3/2\rangle$ + 5.4% $ \pm 1/2\rangle$
KD3	40.0% $ \pm 3/2\rangle$ + 32.9% $ \pm 1/2\rangle$ + 7.9% $ \pm 7/2\rangle$ + 6.5% $ \pm 5/2\rangle$
KD4	19.7% $ \pm 5/2\rangle$ + 16.4% $ \pm 7/2\rangle$ + 9.1% $ \pm 1/2\rangle$ + 8.7% $ \pm 3/2\rangle$
KD5	37.9% $ \pm 1/2\rangle$ + 25.1% $ \pm 9/2\rangle$ + 23.7% $ \pm 3/2\rangle$ + 1.8% $ \pm 5/2\rangle$
4-Sm	
KD1	35.1% $ \pm 1/2\rangle$ + 29.2% $ \pm 3/2\rangle$ + 20.2% $ \pm 5/2\rangle$
KD2	36.8% $ \pm 3/2\rangle$ + 35.7% $ \pm 5/2\rangle$ + 1.3% $ \pm 1/2\rangle$
KD3	31.8% $ \pm 5/2\rangle$ + 18.5% $ \pm 3/2\rangle$ + 12.0% $ \pm 1/2\rangle$
5-Tb	

1	50.0% $ \pm 6\rangle + 0.7\% \pm 2\rangle + 0.5\% \pm 3\rangle + 0.2\% \pm 4\rangle + 0.1\% \pm 1\rangle$
2	49.5% $ \pm 5\rangle + 3.1\% \pm 3\rangle + 1.6\% \pm 4\rangle + 1.2\% \pm 0\rangle + 0.8\% \pm 1\rangle$
3	49.0% $ \pm 4\rangle + 6.8\% \pm 1\rangle + 5.8\% \pm 3\rangle + 2.1\% \pm 0\rangle + 1.5\% \pm 5\rangle$
4	31.5% $ \pm 2\rangle + 26.3\% \pm 1\rangle + 20.3\% \pm 3\rangle + 8.5\% \pm 2\rangle + 2.6\% \pm 4\rangle$
5	28.9% $ \pm 3\rangle + 19.6\% \pm 1\rangle + 14.7\% 0\rangle + 14.2\% \pm 2\rangle + 0.09\% \pm 5\rangle$
6	45.6% $ \pm 1\rangle + 22.6\% \pm 2\rangle + 3.4\% \pm 3\rangle + 0.2\% \pm 4\rangle$
6-Dy	
KD1	95.6% $ \pm 15/2\rangle + 1.7\% \pm 11/2\rangle + 1.1\% \pm 9/2\rangle + 0.4\% \pm 13/2\rangle$
KD2	76.7% $ \pm 13/2\rangle + 10.2\% \pm 11/2\rangle + 10.0\% \pm 9/2\rangle + 2.7\% \pm 7/2\rangle$
KD3	63.8% $ \pm 11/2\rangle + 17.1\% \pm 7/2\rangle + 3.8\% \pm 15/2\rangle + 1.4\% \pm 5/2\rangle$
KD4	66.1% $ \pm 9/2\rangle + 15.5\% \pm 5/2\rangle + 12.9\% \pm 13/2\rangle + 2.8\% \pm 11/2\rangle$
KD5	64.5% $ \pm 7/2\rangle + 18.5\% \pm 11/2\rangle + 7.5\% \pm 3/2\rangle + 2.1\% \pm 1/2\rangle$
KD6	51.8% $ \pm 5/2\rangle + 5.0\% \pm 3/2\rangle + 4.8\% \pm 1/2\rangle + 3.1\% \pm 9/2\rangle$
KD7	52.8% $ \pm 3/2\rangle + 12.1\% \pm 1/2\rangle + 8.0\% \pm 5/2\rangle + 3.5\% \pm 9/2\rangle$
KD8	47.6% $ \pm 1/2\rangle + 10.1\% \pm 3/2\rangle + 4.2\% \pm 7/2\rangle + 0.3\% \pm 11/2\rangle$

TableS10. SINGLE_ANISO computed crystal field parameter (B_k^q) for **2-Ce-6-Dy**. The major components in the Table are in bold.

		2-Ce	3-Nd	4-Sm	5-Tb	6-Dy
k	q	B_k^q	B_k^q	B_k^q	B_k^q	B_k^q
2	-2	-0.12E+02	0.28E+01	0.15E+01	-0.17E+01	0.15E-02
	-1	-0.27E+01	-0.34E+01	-0.11E+02	-0.56E-01	0.78E-01
	0	-0.28E+01	-0.21E+01	0.91E+00	-0.50E+01	-0.29E+01
	1	0.17E+00	0.29E+01	0.63E+00	0.35E+00	-0.13E-03
	2	-0.44E+01	0.39E+00	-0.34E+02	-0.73E+00	0.11E+01
4	-4	0.11E+00	-0.29E-01	-0.14E+00	0.60E-02	0.18E-04
	-3	0.51E+01	-0.12E+00	-0.79E+01	0.65E-01	0.32E-01
	-2	0.20E+01	0.31E-01	-0.59E-01	0.29E-01	0.35E-04
	-1	0.11E+00	0.13E+00	0.20E+01	0.12E-02	0.42E-02
	0	-0.45E+01	0.89E-02	0.15E+00	-0.33E-02	0.27E-02
	1	-0.18E-01	-0.10E+00	0.476E-01	-0.29E-02	-0.26E-04
	2	0.96E+00	0.36E-02	-0.81E+00	0.12E-01	0.12E-01
	3	-0.27E+01	-0.25E+00	-0.99E+00	-0.20E-01	-0.13E-03

	4	-0.47E-01	0.58E-01	0.60E+00	-0.64E-02	-0.30E-02
6	-6		-0.11E-03		0.52E-06	0.23E-06
	-5		0.23E-01		0.59E-04	-0.67E-04
	-4		-0.64E-02		-0.15E-03	0.14E-05
	-3		-0.93E-02		-0.50E-03	-0.43E-03
	-2		0.87E-03		-0.47E-03	-0.95E-06
	-1		0.18E-01		-0.39E-04	-0.22E-04
	0		-0.16E-03		0.38E-04	-0.34E-04
	1		-0.16E-01		-0.48E-04	-0.43E-06
	2		-0.52E-03		-0.18E-03	-0.36E-03
	3		-0.23E-01		0.14E-03	0.12E-05
	4		0.14E-01		0.17E-03	0.19E-03
	5		-0.32E-02		-0.59E-04	-0.22E-06
	6		0.23E-03		-0.99E-04	0.52E-04

Table S11. SINGLE_ANISO computed g -values, the angle of deviation (θ) from ground state g_{zz} orientation of low-lying Kramers doublet for Nd^{III} and Sm^{III} ions in complexes **3-Nd**-**4-Sm** and tunneling splitting Δ_{tun} (for non KDs of Tb^{III} in complex **5-Tb**) in cm⁻¹ respectively.

2-Ce		
$\pm m_J$ states (from 7 Doublets)	$g_{xx}; g_{yy}; g_{zz}$	θ ($^{\circ}$ angle)
0.000	0.0758; 0.1306; 4.0888	0.0
363.828	1.0493; 1.2945; 3.4315	98.5
583.392	0.1210; 0.9332; 3.5225	91.2
3-Nd		
$\pm m_J$ states (from 35 Quartets + 112 Doublets)	$g_{xx}; g_{yy}; g_{zz}$	θ ($^{\circ}$ angle)
0.000	0.151; 0.255; 4.865	0.0
31.601	0.0226; 0.221; 5.892	141.5
148.954	0.198; 0.594; 3.9097	79.5
403.028	3.845; 3.213; 0.549	134.1
428.000	0.271; 0.840; 5.135	125.4
4-Sm		
$\pm m_J$ states (from 21 Sextets + 128 Quartets)	$g_{xx}; g_{yy}; g_{zz}$	θ ($^{\circ}$ angle)
0.000	0.857; 0.795; 0.103	0.0
170.662	0.082; 0.116; 1.511	44.0
417.211	0.036; 0.137; 2.038	97.2
5-Tb		

$\pm m_J$ states (from 7 Septets + 140 Quintets)	$g_{xx}; g_{yy}; g_{zz}$	Δ_{tun}
0.000	0.000; 0.000; 17.999	0.002
176.983	0.000; 0.000; 14.756	0.030
331.466	0.000; 0.000; 11.359	3.260
407.565	0.000; 0.000; 12.211	19.070
450.353	0.000; 0.000; 4.850	18.362
624.680	0.000; 0.000; 17.426	3.260

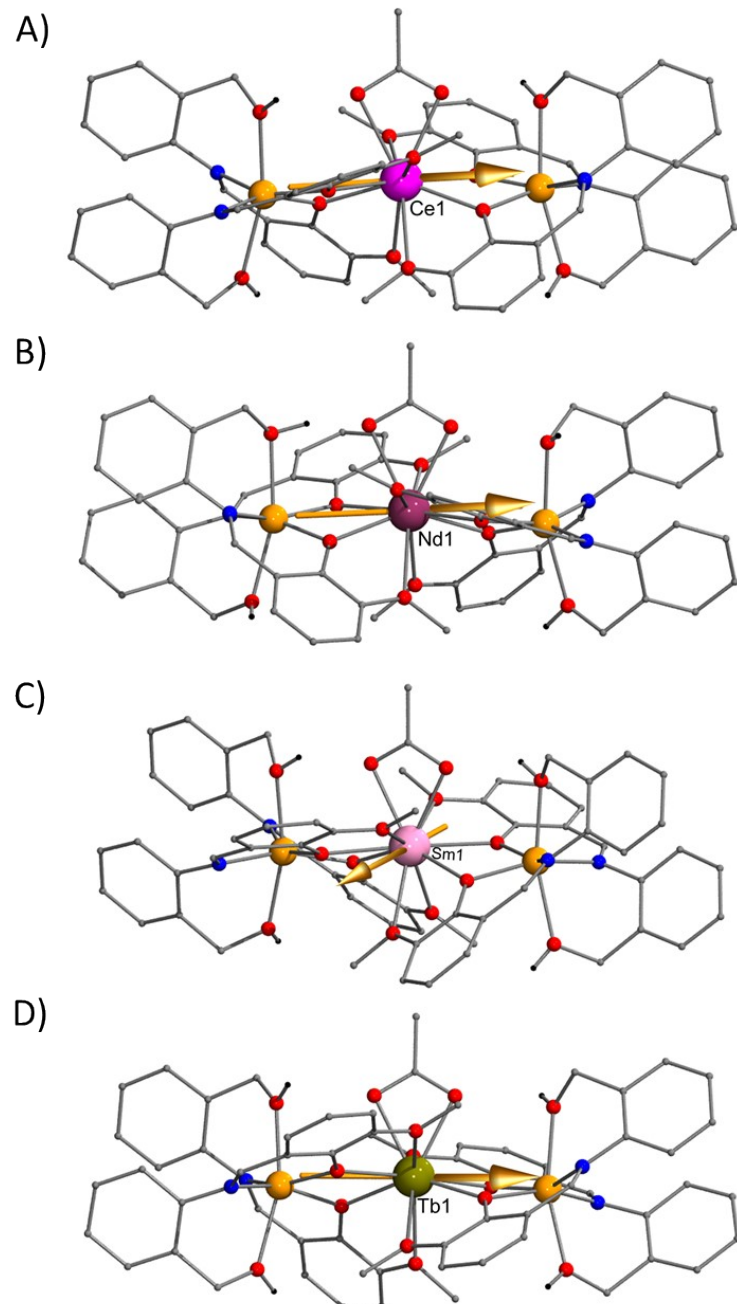


Figure S7. The orientation of computed ground state g_{zz} axis (A-D) in complexes **2-Ce-5-Tb** respectively

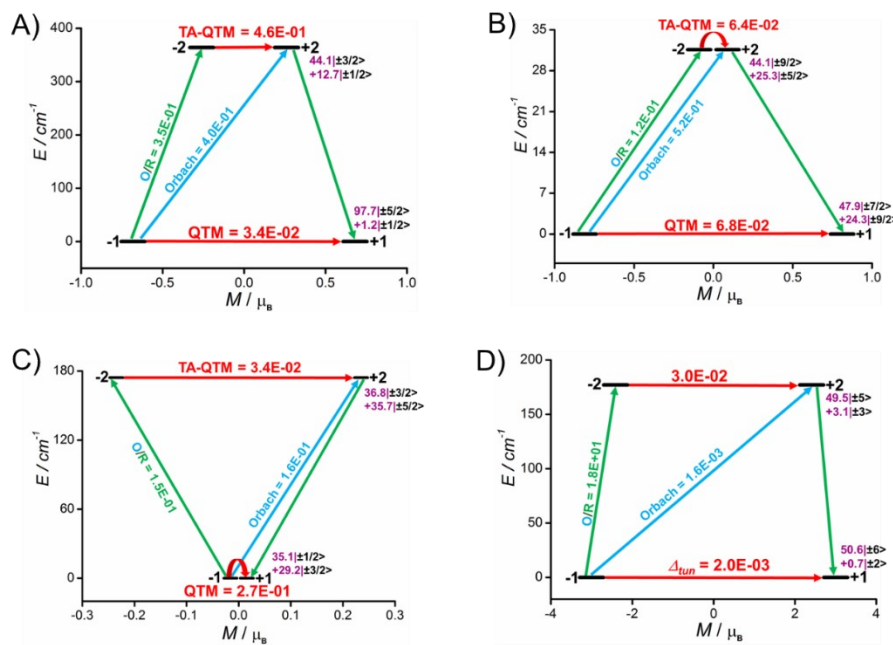


Figure S8. The computed magnetic relaxation mechanism (A-D) for complexes **2-Ce-5-Tb**.

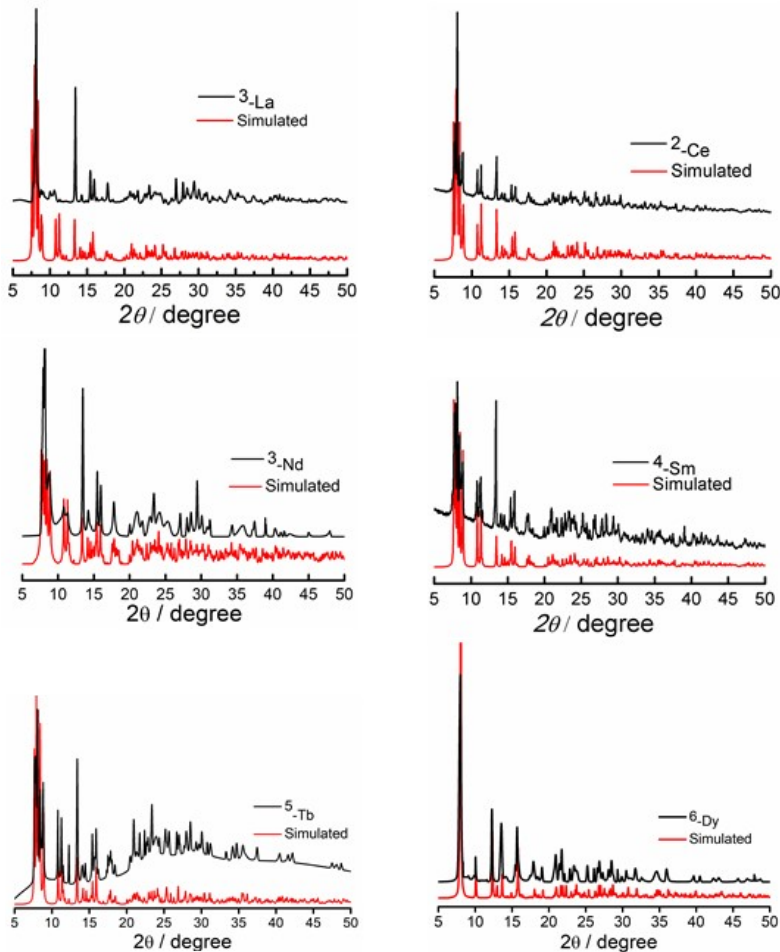


Figure S9. Powder X-ray of the compexes **1-La** – **6-Dy**. The red solid line represent the simulated spectra and black solid line represents the experiment spectra.

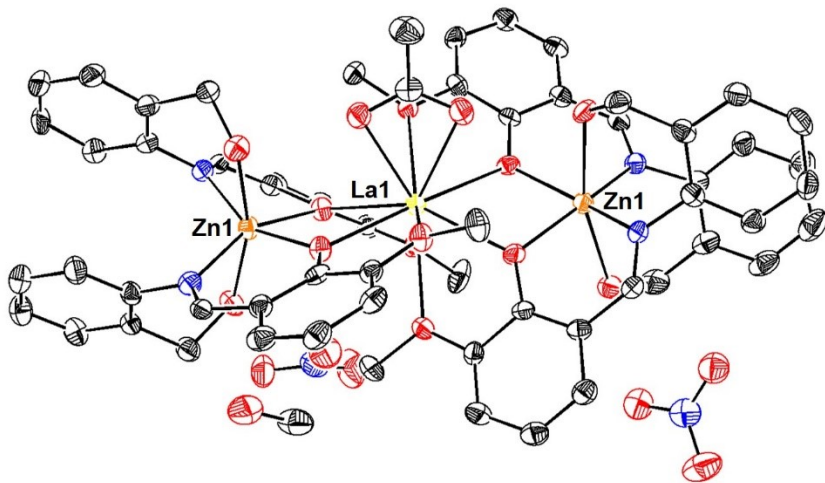


Figure S10. ORTEP diagram of complex $\mathbf{1}_{\text{La}}$, Color code: Red = oxygen, Blue = nitrogen, Black = Carbon, Yellow = lanthanum

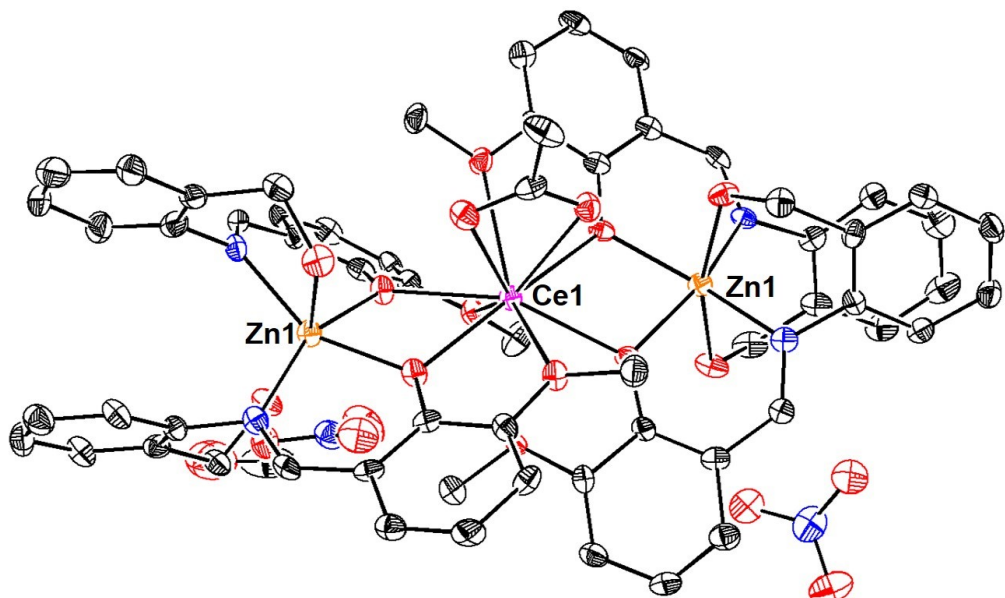


Figure S11. ORTEP diagram of complex $\mathbf{2}_{\text{Ce}}$, Color code: Red = oxygen, Blue = nitrogen, Black = Carbon, Magenta = Cerium

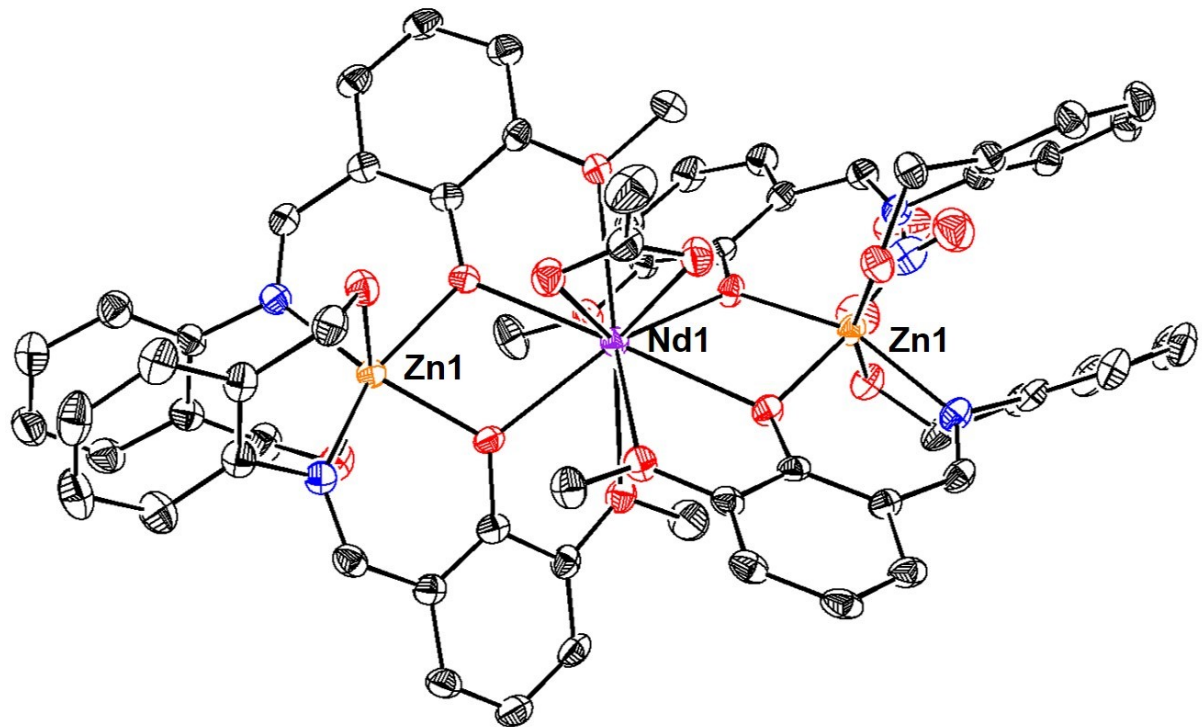


Figure S12. ORTEP diagram of complex 3_{Nd} , Color code: Red = oxygen, Blue = nitrogen, Black = Carbon, Purple = Neodymium

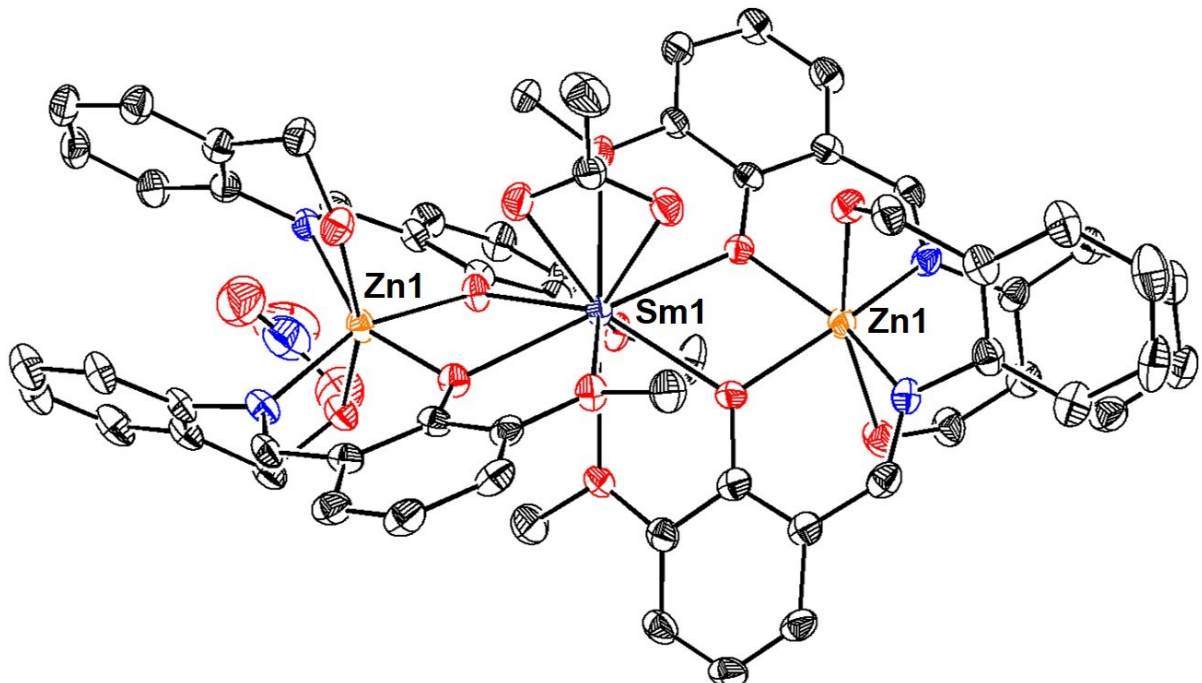


Figure S13. ORTEP diagram of complex 4_{Sm} , Color code: Red = oxygen, Blue = nitrogen, Black = Carbon, Navy blue = Samarium

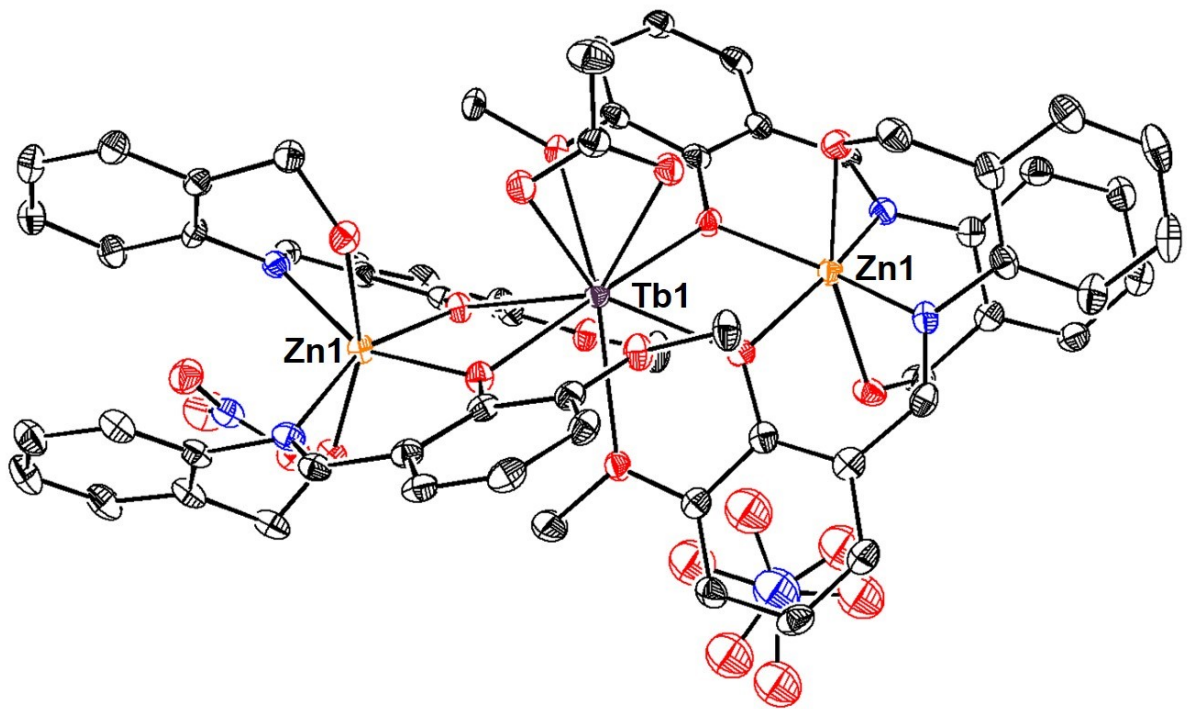


Figure S14. ORTEP diagram of complex $\mathbf{5}_{\text{Tb}}$, Color code: Red = oxygen, Blue = nitrogen, Black = Carbon, Violet= Terbium

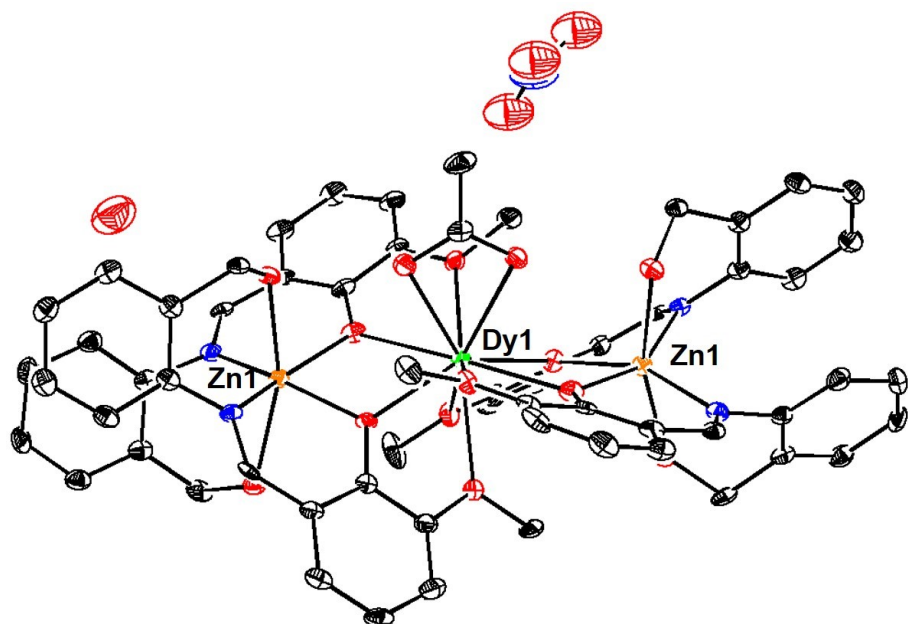


Figure S15. ORTEP diagram of complex $\mathbf{6}_{\text{Dy}}$, Color code: Red = oxygen, Blue = nitrogen, Black = Carbon, Green = Dysprosium

References

1. P.-Y. Shan, H.-F. Li, P. Chen, Y.-M. Tian, W.-B. Sun and P.-F. Yan, *Zeitschrift für anorganische und allgemeine Chemie*, 2015, 641, 1119-1124.
2. J. P. Costes, S. Titos-Padilla, I. Oyarzabal, T. Gupta, C. Duhayon, G. Rajaraman and E. Colacio, *Chemistry – A European Journal*, 2015, 21, 15785-15796.
3. W.-B. Sun, P.-F. Yan, S.-D. Jiang, B.-W. Wang, Y.-Q. Zhang, H.-F. Li, P. Chen, Z.-M. Wang and S. Gao, *Chemical Science*, 2016, 7, 684-691.
4. M. Li, H. Wu, Q. Wei, H. Ke, B. Yin, S. Zhang, X. Lv, G. Xie and S. Chen, *Dalton Transactions*, 2018, 47, 9482-9491.
5. P. Shukla, K. U. Ansari, C. Gao, S. Vaidya, S. Tripathi, P. Kumar, R. J. Butcher, J. Overgaard and M. Shanmugam, *Dalton Transactions*, 2020, 49, 10580-10593.